JCTC Journal of Chemical Theory and Computation

Article

Cite This: J. Chem. Theory Comput. 2019, 15, 3844−3853

pubs.acs.org/JCTC

Configurational Entropy Components and Their Contribution to Biomolecular Complex Formation

Markus Fleck[†,‡] and Bojan Zagrovic*[,†]

[†]University of Vienna, Max F. Perutz Laboratories, Department of Structural and Computational Biology, Campus Vienna Biocenter 5, Vienna 1030, Austria

[‡]University of Vienna, Faculty of Chemistry, Department of Computational Biological Chemistry, Währinger Straße 17, Vienna 1090, Austria

Supporting Information

ABSTRACT: Configurational entropy change is a central constituent of the free energy change in noncovalent interactions between biomolecules. Due to both experimental and computational limitations, however, the impact of individual contributions to configurational entropy change remains underexplored. Here, we develop a novel, fully analytical framework to dissect the configurational entropy change of binding into contributions coming from molecular internal and external degrees of freedom. Importantly, this framework accounts for all coupled and uncoupled contributions in the absence of an external field. We employ our parallel implementation of the maximum information spanning tree algorithm to provide a comprehensive numerical analysis of the importance of the individual contributions to configurational entropy change on an extensive set of molecular dynamics simulations of protein binding processes. Contrary to commonly accepted assumptions, we show that different coupling terms contribute significantly to the overall configurational entropy change. Finally, while the magnitude of individual terms may be largely unpredictable a priori, the total configurational entropy change can be well approximated by rescaling the sum of uncoupled contributions from internal degrees of freedom only, providing support for NMR-based approaches for configurational entropy change estimation.

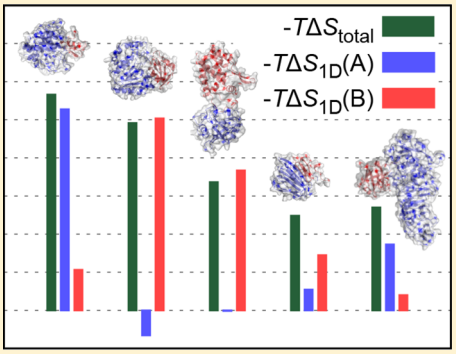

1. INTRODUCTION

Noncovalent interactions between macromolecules are fundamental to a large number of biological processes including transcription, translation, cell signaling, and many other.[1] Given an isothermal−isobaric ensemble with a constant number of particles (NPT), the Gibbs free energy change [see, e.g., ref 2]

$$\Delta G_{\text{system}} = \Delta H_{\text{system}} - T\Delta S_{\text{system}} \quad (1)$$

captures the likelihood for such a binding process to occur, together with the equilibrium fractions of the species involved. Importantly, the entropic term ($-T\Delta S_{\text{system}}$) remains largely underexplored when it comes to biological macromolecules. This especially concerns the configurational entropy part of the total entropy change, which stems from the solute degrees of freedom only and is notoriously difficult to measure experimentally[3−5] or calculate from atomistic simulations.[6−18] It has traditionally been assumed that the configurational entropy change is negligible in comparison to the change in solvent entropy.[19] Recently, however, it was experimentally demonstrated that the configurational entropy contribution in the case of proteins can be of similar magnitude as the solvent entropy contribution[3−5] and can thus potentially have a strong impact on the thermodynamics of protein interactions. In a more applied context, deeper insight into configurational entropy and the basic physical principles that govern its response to changes in biomolecular dynamics could significantly improve computational drug design by helping to overcome enthalpy/entropy compensation.[20−22] In the present work, we analyze the individual contributions to configurational entropy change of protein binding, stemming from internal[12,23−28] and external (rigid body rototranslational) degrees of freedom. Going beyond the previous studies of entropy change in protein−protein interactions, such as those involving normal mode calculations,[29,30] we investigate here the importance and the relative magnitude of the often ignored coupling (correlation) terms between internal and external degrees of freedom in BAT coordinates. Following previous work,[31] we employ an entropy decomposition[32] known as the mutual information expansion (MIE) in its analytical form. There exists a well-developed theoretical apparatus for the decomposition of such coupling terms (see, e.g., refs 12 and 33 and references therein), mainly for liquids. However, numerical application of MIE as an approximation of the configurational entropy is rather novel in the case of configurational entropy of biomolecules.[12]

Received: December 13, 2018
Published: May 1, 2019

DOI: 10.1021/acs.jctc.8b01254
J. Chem. Theory Comput. 2019, 15, 3844−3853

In the pioneering work by Gilson and co-workers,[12] the MIE expansion is taken at the level of single degrees of freedom as opposed to sets of degrees of freedom, which, as mentioned above, will be treated in this work. The obtained numerical coupling terms can then be summed up to approximate the analytical MIE coupling terms at the level of the sets of degrees of freedom, e.g., external with internal or main-chain with side-chain. In this context, Gilson and co-workers[34] have recently discussed and reviewed the general significance of coupling corrections in configurational entropy estimation. Importantly, they have applied a more recently developed variant of the MIE approximation, the maximum information spanning tree (MIST) approximation.[10,35] However, MIST/MIE analysis of the coupling terms in proteins resulting from the partitioning into external and internal degrees of freedom is, to the best of our knowledge, limited to a single case study,[11] employing the MIE approximation at pairwise order.

Here, by distilling the previous work[31,32] to a compact form, we arrive at a decomposition of entropy into sets of external and internal degrees of freedom in the form of a general framework, which takes advantage of separable terms in the underlying potential energy. We compute these contributions to configurational entropy change at pairwise order for a large set of typical protein complexes (Figure 1 and Table 1). The isolated binding partners and their binary complexes are captured using microsecond-level classical molecular dynamics simulations (for methodological details and a full description of the simulated set, please see refs 36−38). The simulated set exhibits a wide range of physical sizes and secondary- and tertiary-structure classes of individual binding partners as well as a variety of the total configurational entropy changes and the uncoupled configurational entropy changes of individual binding partners. Note that five of the simulated complexes involve ubiquitin as one of the binding partners (Figure 1a), a well-folded, biologically important protein frequently used in biophysical studies; we highlight these complexes for clarity in all of our analyses. This large-scale investigation is made possible by our recent parallel implementation[36] of MIE/MIST. For three representative complexes, we carry out an extensive analysis of configurational entropy convergence, leading to several notable results. Additionally, as there exists a certain fundamental arbitrariness[31,39,40] in decomposing the entropy over external and internal degrees of freedom, we provide an analysis of the impact of different decomposition choices (Figure 5). We demonstrate that several coupling terms contribute significantly to the overall configurational entropy change across different proteins, contrary to commonly accepted assumptions. Finally, we provide a justification for the experimental estimation of the total entropy change from the leading internal uncoupled entropy terms even under these circumstances.

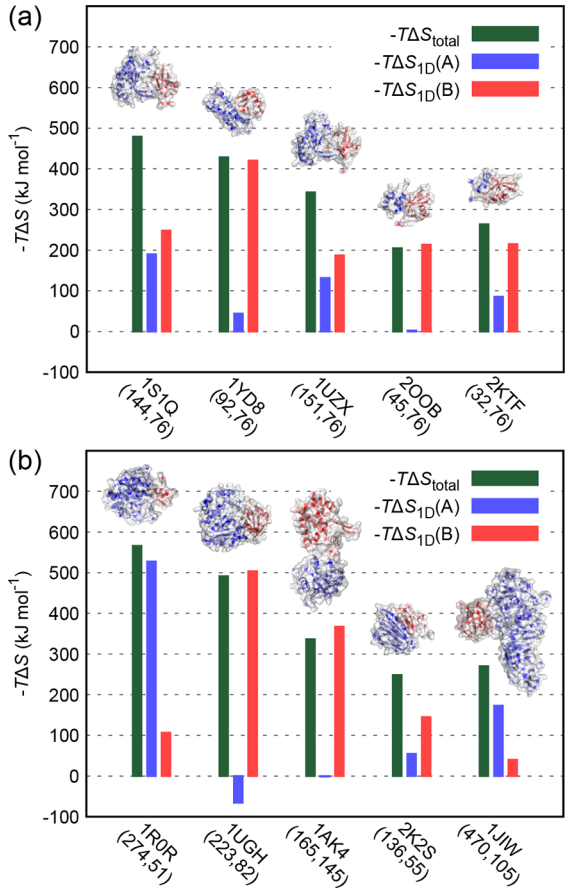

Figure 1. Structures of the simulated protein complexes together with the computed configurational entropy contributions to the Gibb's free energy change of binding of the whole complexes ($-T\Delta S_{total}$) or binding partners alone [$-T\Delta S_{1D}(A)$ and $-T\Delta S_{1D}(B)$]. The latter values stem from the internal degrees of freedom of individual binding partners without any coupling (mutual information) contributions included. On the *x*-axis, we give the PDB code[41,42] of each complex together with the number of amino acids in each partner (in parentheses). In (a), the second binding partner B (colored red) is always ubiquitin. Please see Table 1 for further details concerning the simulated complexes.

2. THEORY

2.1. Configurational Entropy of the Binding Process.

An expression for the configurational entropy of a single molecule or complex can be derived from the quasi-classical entropy integral[43,44]

$$S_{solute} = -R \int d\vec{q}\; d\vec{p}\; \rho(\vec{q}, \vec{p})\, \ln[h^{3N}\rho(\vec{q}, \vec{p})] \tag{2}$$

where R represents the universal gas constant, h the Planck constant, N the number of atoms in the molecule, and ρ the classical phase-space probability density function (pdf). $\vec{q}$ and $\vec{p}$ denote, respectively, the spatial degrees of freedom and the canonically conjugate momenta in Cartesian coordinates. Note that due to the factor h^{3N} this integral cannot be split into momentum and spatial parts while preserving physically correct dimensions for both quantities.[38,43] As in this work we are concerned with the spatial part of the entropy (labeled just S to simplify the notation), a convenient choice for separating off the momentum entropy S_m is

$$\begin{aligned} S_{solute} &= S + S_m \\ S &= -R \int d\vec{q}\; \rho(\vec{q})\, \ln[\rho(\vec{p})] \\ S_m &= -R \int d\vec{p}\; \rho(\vec{p})\, \ln[h^{3N}\rho(\vec{p})] \end{aligned} \tag{3}$$

The momentum entropy then evaluates to[38,43]

$$S_m = R\frac{3N}{2}\left[1 + \ln\left(2\pi\left(\prod_{i=1}^{3N} m_i\right)^{1/(3N)} k_B T\right)\right] - R\ln(h^{3N}) \tag{4}$$

DOI: 10.1021/acs.jctc.8b01254
J. Chem. Theory Comput. 2019, 15, 3844−3853

Table 1. Simulated Protein Set

name	# atoms[a]	PDB code[b]	complex[c]	$-T\Delta S_{1D}$[d]
Tsg101 protein	1480	1KPP	1S1Q	190.0
ubiquitin	760	1UBQ	1S1Q	248.3
gGGA3 Gat domain[e]	949	1YD8*	1YD8	44.0
ubiquitin	760	1UBQ	1YD8	420.4
ESCRT-I complex subunit VPS23	1493	3R3Q	1UZX	131.6
ubiquitin	760	1UBQ	1UZX	187.5
E3 ubiquitin−protein ligase CBL-B	457	2OOA	2OOB	2.4
ubiquitin	760	1UBQ	2OOB	213.5
polymerase iota ubiquitin-binding motif	457	2L0G	2KTF	85.5
ubiquitin	760	1UBQ	2KTF	215.1
subtilisin Carlsberg	2433	1SCD	1R0R	527.4
ovomucoid	498	2GKR	1R0R	106.6
uracil−DNA glycosylase	2333	1AKZ	1UGH	−65.7
uracil−DNA glycosylase inhibitor	788	1UGI	1UGH	503.8
PPIase A	1641	1W8V	1AK4	−1.4
PR160Gag-Pol	1408	2PXR	1AK4	367.4
micronemal protein 1	1226	2BVB	2K2S	54.5
micronemal protein 6	496	2K2T	2K2S	145.0
alkaline protease	4503	1AKL	1JIW	173.1
alkaline protease inhibitor	997	2RN4	1JIW	40.0

[a]Number of force field atoms of individual proteins. [b]PDB codes[41,42] of individual proteins. [c]PDB codes of complexes. [d]Entropy change from internal degrees of freedom of individual binding partners upon complex formation without any coupling (mutual information) contributions, given in kJ mol^{-1}, as in Figure 1. [e]The constituent GGA3 Gat domain was extracted from the PDB structure of the 1YD8 complex and named 1YD8* accordingly.

Here, m_i denotes the mass vector of the solute, and k_B is the Boltzmann constant. Note that this expression is constant if the temperature and atomic composition remain fixed. Under the assumption of a vanishing external field and a concentration C° associated with a container of volume $V^\circ = 1/C^\circ$ for a single molecule (or complex), the spatial part of eq 2 can be evaluated to[11,12,43]

$$S = R\ln(8\pi^2 V^\circ) - R\int \mathrm{d}\vec{q}_{\mathrm{int}}\, J(\vec{q}_{\mathrm{int}})\rho(\vec{q}_{\mathrm{int}})\ln[\rho(\vec{q}_{\mathrm{int}})] \equiv S_{\mathrm{conf}}^{\mathrm{ext}} + S_{\mathrm{conf}}^{\mathrm{int}} \tag{5}$$

where $J(\vec{q}_{\mathrm{int}})$ denotes the Jacobian of the chosen molecule internal coordinates (such as anchored Cartesian[23,24] or BAT[12,23−28] coordinates). Thus, the second term on the right-hand side captures the integration over the chosen $3N-6$ internal degrees of freedom $\vec{q}_{\mathrm{int}}$. The term $R\ln(8\pi^2V^\circ)$ in eq 5 results from integration over the 6 external degrees of freedom, which in the absence of an external field can be carried out analytically.[26] Here, following a common practice, we choose a standard concentration of $C^\circ = 1/V^\circ = 1\ \mathrm{mol\ L^{-3}}$. As this term as well as the momentum entropy at fixed temperature and atomic composition is constant,[38,43] the second term on the right-hand side of eq 5 alone is often referred to as configurational entropy. Therefore, for a single molecule, sampling the internal, spatial pdfs is sufficient to calculate the total entropy contribution to the Gibbs free energy change from the solute. Importantly, while neither the momentum entropy (eq 4) nor the spatial entropy (eq 5), as mentioned above, exhibit physically correct dimensions, the problematic terms cancel for entropy differences.[38,43] Thus, differences (and differences only) of these quantities bear physically valid dimensions of entropy.

We now begin our analysis of the configurational entropy change of a binary binding process by deriving the configurational entropy of the unbound state (including external degrees of freedom), followed by the derivation of the configurational entropy of the bound state. As mentioned in the introduction, both derivations follow a previously discussed strategy,[31] making extensive use of the analytical MIE.[32] The configurational entropy change upon binding is then obtained by subtraction. As no other approximations are made apart from the assumption of a vanishing external field, the end result as well as all intermediate results are analytically exact in the classical limit.

2.2. Configurational Entropy of the Unbound State from a Statistical-Mechanical Perspective. In the unbound state, the molecules are assumed to be infinitely far apart, and we assume no external fields. The notation used for describing different terms is given in Table 2. Note that from now on we drop the vector symbol for a more convenient notation. With these assumptions and notation, the potential energy separates as

Table 2. Nomenclature of the Degrees of Freedom

q_X	external degrees of freedom molecule 1
q_Y	external degrees of freedom molecule 2[a]
q_A	internal degrees of freedom molecule 1
q_B	internal degrees of freedom molecule 2
X	random variables from q_X
Y	random variables from q_Y
A	random variables from q_A
B	random variables from q_B
$\sim$	a quantity associated with the bound state
S_{1D}	entropy from marginal 1D probability density functions only (within a given subsystem)
I_{2D}	mutual information of 2D and higher probability density functions (within a given subsystem[b])
I_2	pairwise mutual information of 2D and higher probability density functions (shared between two subsystems[b])
I_3	triplet mutual information of 3D and higher probability density functions (shared between three subsystems[c])

[a]In the reference frame of molecule 1. [b]Numerically approximated by 2D probability density functions in this work. [c]Not treated numerically in this work.

$$U(q_X, q_A, q_Y, q_B) = U(q_X) + U(q_A) + U(q_Y) + U(q_B) = U(q_A) + U(q_B) \tag{6}$$

Here, without a loss of generality, the external potential constants are set to zero. Analogously, the pdf factorizes into

$$\rho(q_X, q_A, q_Y, q_B) = \rho(q_X)\rho(q_A)\rho(q_Y)\rho(q_B) = \frac{1}{8\pi^2V^\circ}\rho(q_A)\frac{1}{8\pi^2V^\circ}\rho(q_B) \tag{7}$$

The factor $8\pi^2V^\circ$ results from the homogeneous probability distribution with respect to the position in the container volume, the full solid angle, as well as the external torsional

DOI: 10.1021/acs.jctc.8b01254
J. Chem. Theory Comput. 2019, 15, 3844−3853

degree of freedom of the molecules. Finally, using the corresponding external entropy terms $R\ln(8\pi^2V^\circ)$ from eq 5 and the notation of Table 2, the spatial entropy of the unbound state is given as

$$\begin{aligned} S(X, A, Y, B) &= S(X) + S(A) + S(Y) + S(B) \\ &= S(A) + S(B) + 2R\ln(8\pi^2V^\circ) \end{aligned} \tag{8}$$

2.3. Configurational Entropy of the Unbound State from an Information-Theoretic Perspective. The same result from the previous subsection can be derived in an information-theoretic framework. First, the MIE is denoted as[32]

$$S(X_1, ..., X_n) = \sum_{k=1}^{n} (-1)^{k+1} \sum_{i_1<\cdots<i_k} I_k(X_{i_1}, ..., X_{i_k}) \tag{9}$$

where

$$I_n(X_1, ..., X_n) = \sum_{k=1}^{n} (-1)^{k+1} \sum_{i_1<\cdots<i_k} S(X_{i_1}, ..., X_{i_k}) \tag{10}$$

are the so-called higher-order mutual information (MI) terms of order n. Note however that $I_1(X_i) = S(X_i)$. For further derivation, it will be convenient to first prove the following summary of the previous work[32] in a general form

$$\begin{aligned} &U(q_1, ..., q_N) = U(q_1) + U(q_2, ..., q_N) \\ &\Rightarrow I_k(X_1, X_{i_1}, ..., X_{i_{k-1}}) = 0 \qquad \forall\, k \geq 2 \end{aligned} \tag{11}$$

Here, for every set of degrees of freedom q_i, X_i denotes the corresponding random variable. This equation states that, if a given set of degrees of freedom can be separated out in the energy function, all (higher-order) MI terms describing the coupling of this set to any possible subset (including the full set) of the remaining degrees of freedom vanishes simultaneously. The proof then proceeds as follows. Analogously to eqs 6−8, we have

$$\begin{aligned} &U(q_1, ..., q_N) = U(q_1) + U(q_2, ..., q_N) \\ &\Rightarrow \rho(q_1, ..., q_N) = \rho(q_1) + \rho(q_2, ..., q_N) \\ &\Rightarrow S(X_1, ..., X_N) = S(X_1) + S(X_2, ..., X_N) \end{aligned} \tag{12}$$

Then, from eq 10, it follows for the pairwise MI

$$\begin{aligned} &I_2(X_1, X_2 ... X_N) \\ &= S(X_1) + S(X_2, ..., X_N) - S(X_1, ..., X_N) \\ &= 0 \end{aligned} \tag{13}$$

As for pairwise MI, we have[45]

$$0 \leq I_2(X_1, X_2 ... X_{k-1}X_{k+1}X_N) \leq I_2(X_1, X_2 ... X_N) \tag{14}$$

All pairwise combinations involving X_1 vanish simultaneously. Furthermore, all higher-order MI terms can be expanded recursively as a sum of such vanishing pairwise MI combinations with X_1 using[32]

$$\begin{aligned} I_n(X_1, ..., X_n) = {} & I_{n-1}(X_1, ..., X_{n-2}, X_{n-1}) \\ & + I_{n-1}(X_1, ..., X_{n-2}, X_n) \\ & - I_{n-1}(X_1, ..., X_{n-2}, X_{n-1}X_n) \end{aligned} \tag{15}$$

This completes the proof of eq 11. Now, applying the MIE (eq 9) for the subsystems treated in this work yields the expansion

$$\begin{aligned} S(X, A, Y, B) = {} & S(X) + S(A) + S(Y) + S(B) \\ & - I_2(X, A) - I_2(X, Y) - I_2(X, B) - I_2(A, Y) \\ & - I_2(A, B) - I_2(Y, B) + I_3(X, A, Y) + I_3(X, A, B) \\ & + I_3(X, Y, B) + I_3(A, Y, B) - I_4(X, A, Y, B) \end{aligned} \tag{16}$$

As, according to eq 6, we have $U(q_X,q_A,q_Y,q_B) = U(q_X) + U(q_A) + U(q_Y) + U(q_B)$, all MI terms vanish for the unbound state. Then, in accordance with eq 8, one obtains

$$\begin{aligned} S(X, A, Y, B) &= S(X) + S(A) + S(Y) + S(B) \\ &= S(A) + S(B) + 2R\ln(8\pi^2V^\circ) \end{aligned} \tag{17}$$

2.4. Configurational Entropy of the Bound State. In the bound state, the two molecules are close together, and therefore, the orientation of molecule 2 with respect to molecule 1 contributes to the potential energy. Because in the bound state the internal degrees of freedom between the molecules also influence each other, only the external degrees of freedom of the first molecule remain separable (as they anchor the whole complex and we assume no external field). Thus, denoting the degrees of freedom in the bound state with a tilde, one can write

$$U(q_{\tilde{X}}, q_{\tilde{A}}, q_{\tilde{Y}}, q_{\tilde{B}}) = U(q_{\tilde{X}}) + U(q_{\tilde{A}}, q_{\tilde{Y}}, q_{\tilde{B}}) \tag{18}$$

Then, using eq 11 for the vanishing MI terms and the MIE for the present subsystems (see eq 16), together with the fact that as before $S(\tilde{X}) = R\ln(8\pi^2V^\circ)$, the configurational entropy in the bound state can be written as

$$\begin{aligned} S(\tilde{X}, \tilde{A}, \tilde{Y}, \tilde{B}) = {} & R\ln(8\pi^2V^\circ) + S(\tilde{A}) + S(\tilde{Y}) + S(\tilde{B}) \\ & - I_2(\tilde{A}, \tilde{Y}) - I_2(\tilde{A}, \tilde{B}) - I_2(\tilde{Y}, \tilde{B}) + I_3(\tilde{A}, \tilde{Y}, \tilde{B}) \end{aligned} \tag{19}$$

Note that the same result could be derived by using $S(\tilde{X},\tilde{A},\tilde{Y},\tilde{B}) = S(\tilde{X}) + S(\tilde{A},\tilde{Y},\tilde{B})$ from the statistical mechanical framework due to eq 18 and then applying the MIE (eq 9) just to $S(\tilde{A},\tilde{Y},\tilde{B})$.

2.5. Configurational entropy change upon binding. Using the results from the previous subsections, the configurational entropy change upon binding can be obtained by subtracting eq 17 (or equivalently eq 8) from eq 19 as

$$\begin{aligned} \Delta S = {} & [S(\tilde{A}) - S(A)] + [S(\tilde{B}) - S(B)] \\ & + [S(\tilde{Y}) - \ln(8\pi^2V^\circ)] - I_2(\tilde{A}, \tilde{Y}) - I_2(\tilde{A}, \tilde{B}) \\ & - I_2(\tilde{Y}, \tilde{B}) + I_3(\tilde{A}, \tilde{Y}, \tilde{B}) \\ \equiv {} & \Delta S(A) + \Delta S(B) + \Delta S(Y) - I_2(\tilde{A}, \tilde{Y}) - I_2(\tilde{A}, \tilde{B}) \\ & - I_2(\tilde{Y}, \tilde{B}) + I_3(\tilde{A}, \tilde{Y}, \tilde{B}) \end{aligned} \tag{20}$$

This final result describes the fully analytical configurational entropy change in the absence of an external field expressed in terms of contributions from external and internal degrees of freedom of the molecules involved. It follows from the singular assumption of the form of the potential energy function in eqs 6 and 18 in the classical limit without any further approximations. For the external degrees of freedom of the second molecule, the term $\Delta S(Y) = S(\tilde{Y}) - \ln(8\pi^2V^\circ)$ expresses the rototranslational restriction upon binding to the first molecule, in contrast to the motional freedom in the unbound state. Note also that the only contributions that

DOI: 10.1021/acs.jctc.8b01254
J. Chem. Theory Comput. 2019, 15, 3844−3853

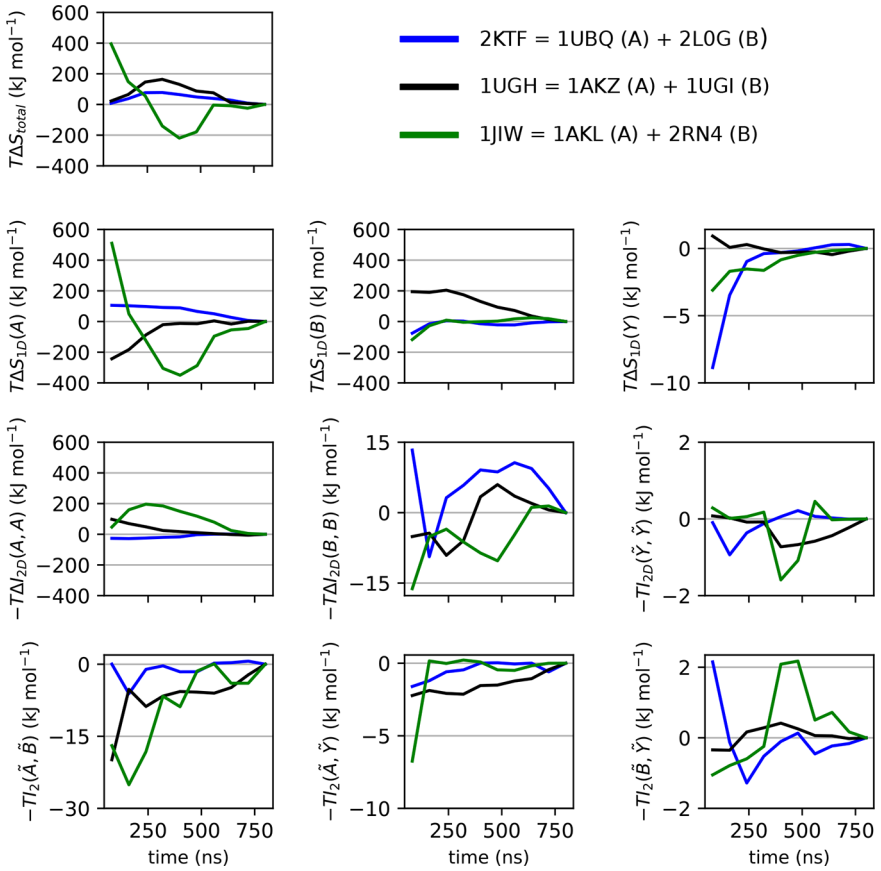

Figure 2. Dependence of the calculated configurational entropy change and its components on simulated time for three representative complexes. For each complex and contribution, we give values based on simulated samples with a 1 ps output frequency whose total size increases incrementally in steps of 80 ns. For visualization purposes, the curves have been shifted to converge to zero when reaching their final value at the total simulation length of 800 ns. The reference to binding partners A and B in different complexes as denoted by their PDB codes is the same as that in Figure 1 and Table 1.

reflect the coupling between the four subsystems stem from the MI in the bound state.

3. RESULTS AND DISCUSSION

Using the above analytical framework, we analyzed the relative importance of the individual contributions to configurational entropy change in the case of 10 protein complexes shown in Figure 1. As a consequence of the limitations of in silico sampling, application of the MIST approximation at an order higher than pairwise is currently not possible for proteins of biologically relevant sizes. However, one can further dissect eq 20 by separating the uncoupled configurational entropy from the mutual information terms within a given subsystem. Here, note that while, e.g., $S(A)$ appears as a one-dimensional term at the level of individual subsystems, when it comes to degrees of freedom, it stems from a high-dimensional probability density function, which one can expand via eq 9. The same holds for I_2 terms: while at the level of individual subsystems they appear as pairwise mutual information terms, at the level of degrees of freedom they are described by higher-order mutual information terms as in eq 9. Separating off the coupling terms within one subsystem leads then to

$$\begin{aligned}\Delta S = {} & \Delta S_{1D}(A) + \Delta S_{1D}(B) + \Delta S_{1D}(Y) \\ & - \Delta I_{2D}(A, A) - \Delta I_{2D}(B, B) - I_{2D}(\tilde{Y}, \tilde{Y}) \\ & - I_2(\tilde{A}, \tilde{Y}) - I_2(\tilde{A}, \tilde{B}) - I_2(\tilde{Y}, \tilde{B}) + I_3(\tilde{A}, \tilde{Y}, \tilde{B})\end{aligned} \tag{21}$$

Here, as denoted in Table 2, S_{1D} refers to the sum of the I_1 terms in eq 9 and I_{2D} to the sum of all terms I_k with $k > 1$, both referring to the equation expressed at the level of degrees of freedom and within one subsystem. While our analysis approximates all I_{2D} and I_2 terms in eq 21 from 2D pdfs over the degrees of freedom, the triplet term I_3 inherently has dimensions ≥ 3 and is, thus, difficult to sample properly. Note that the term $I_{2D}(\tilde{Y},\tilde{Y})$ is zero for the unbound state, corresponding to the total motional freedom of the molecules. Thus, $I_{2D}(\tilde{Y},\tilde{Y})$ enters the equation directly without making a difference in the case of the unbound state.

3.1. Convergence Analysis. Before analyzing and comparing individual contributions to the configurational entropy change, we would first like to discuss the convergence of our computational estimates. The uncertainty in configurational entropy calculations stems, in principle, from two main sources. First, the underlying simulations need to accurately and exhaustively sample the configurational space explored by a given molecule. While the question of force field accuracy is an important one, its adequate treatment is beyond the scope of the present study. On the other hand, the question of how

DOI: 10.1021/acs.jctc.8b01254
J. Chem. Theory Comput. 2019, 15, 3844−3853

exhaustively the phase space is sampled may be addressed by monitoring the convergence of the configurational entropy change and its components as a function of simulated time. Second, uncertainty is also influenced by the intrinsic properties of different configurational entropy components and their dependence on sufficient sample size. This question may be addressed by analyzing samples of different size coming from a shuffled trajectory in which the ordering of individual snapshots is randomized, thus removing the physical sources of uncertainty. We have carried out both of these types of analysis for three representative complexes in our set: the smallest one (PDB code 2KTF), the largest one (PDB code 1JIW), and a medium-size one involving S_{1D} terms with noteworthy properties, as further discussed below (PDB code 1UGH).

When it comes to total entropy change and its convergence as a function of physical time, the complexes converge to within 9, 7, and 25 kJ/mol from the final value for the 2KTF, 1UGH, and 1JIW complexes, respectively, already 80 ns before the end of the simulated trajectories (Figure 2). Considering the configurational entropy components, for 1JIW, the principal determinant of convergence is the $T\Delta S_{1D}$ term of its larger protein 1AKZ, making up 4503 of its total 5500 atoms. The corresponding mutual information term $-T\Delta I_{2D}$, in fact, converges considerably better (Figure 2): for example, over the last 80 ns, $T\Delta S_{1D}$ rises by about 46 kJ mol^{-1}, while $-\Delta I_{2D}$ drops by only 5 kJ mol^{-1}. In fact, an analogues statement can be made for all six proteins analyzed: $-T\Delta I_{2D}$ does not constitute the limiting factor for convergence. It is rather the $T\Delta S_{1D}$ terms that are more problematic to converge. Another noteworthy observation can be made for 1UGH: the larger protein 1AKZ, constituting 2333 of the 3121 atoms, converges surprisingly well in all of its components (Figure 2). The $T\Delta S_{1D}$ terms of the smaller protein 1UGI, on the other hand, still drop by 35 kJ mol^{-1} over the last 160 ns. The reason for this is likely the magnitude of the respective $T\Delta S_{1D}$ values, which is −66 kJ mol^{-1} for 1AKZ and a considerable 504 kJ mol^{-1} for 1UGI after the full 800 ns of the simulations. This suggests that physical size is not necessarily the deciding factor in convergence.

The other terms considered in this study, $T\Delta S_{1D}(Y)$, $-TI_{2D}(\tilde{Y},\tilde{Y})$, $-TI_2(\tilde{A},\tilde{B})$, $-TI_2(\tilde{A},\tilde{Y})$, and $-TI_2(\tilde{B},\tilde{Y})$, show rather satisfactory convergence properties for all complexes analyzed, with their values coming to within approximately 2, 2, 5, 2, and 2 kJ mol^{-1}, respectively, of the final values already in a few 80 ns steps.

What is left to discuss are the convergence properties of 1UBQ in the 2KTF complex. While ubiquitin is a stable, well-folded protein, its configurational entropy converges rather slowly, especially in its $T\Delta S_{1D}$ terms, which still drop by about 27 kJ mol^{-1} over the last 160 ns. The reason for this likely stems from the fact that, while well-folded, ubiquitin explores different conformational substates on a time scale that is slow compared to the simulation length of 800 ns. Indeed, the excellent convergence of configurational entropy changes and their components for all three complexes in the analysis of shuffled trajectories, with all terms converging to within 6 kJ/mol or less from the final value already within the first 80 ns (Figure SI 1), strongly suggests that the key determinant for convergence is not the sheer number of frames used for the configurational entropy calculation, but rather the quality of the underlying coverage of the phase space. In fact, the initial convergence in the analysis of shuffled trajectories turned out to be so rapid for all six proteins of the three complexes studied that we had to fine-grain the first 80 ns to steps of 8 ns to produce SI Figure 1.

Putting the convergence issues aside, the final configurational entropy change values, as calculated here, may seem relatively high. There are three separate issues that need to be mentioned in this regard. First, the MIST approximation is by definition an upper bound on the absolute configurational entropy and, if the underlying absolute values are too high, it is likely that the corresponding differences will show the same trend. Note, however, that when compared to the values obtained by the quasi-harmonic approximation the MIST configurational entropy differences are actually lower by a factor of approximately 3.[38] Next, a large change in entropy is frequently accompanied by a large change in enthalpy, resulting in a moderate value for the relevant free energy change.[3] In this sense, our results could very much be physically meaningful. Finally, the main experimental estimates of configurational entropy changes in protein interactions are derived from the changes in the NMR methyl order parameters by using a linear relationship between the two.[38,46] While the proteins in our set indeed exhibit somewhat higher values of configurational entropy change as compared to the proteins that have been studied experimentally,[46] they also explore a significantly larger range of order parameter changes (a factor of ∼3). Taking this into the account, one could claim that our results are approximately consistent with the experimentally measured magnitude of configurational entropy change.

3.2. Evaluation of Contributions to Configurational Entropy Change. Acknowledging the uncertainties discussed in the previous section, we now turn back to the numerical investigation of eq 21. In Figure 3a, we evaluate this breakdown on our simulated set, each captured by one point in every column, as calculated from the pairwise order MIST approximation. The percentage values given in the graph capture the span of the values in reference to the span of the column ΔS_{total}. Thus, these values can be interpreted as the numerical measure of the importance of a given contribution. We have opted for such a means of comparing different terms because taking the ratios between individual components for the same binding process, while seemingly more natural, results in some cases in misleadingly extreme values. As expected, the 1D terms of the internal degrees of freedom contribute the most, followed by the coupling within the molecules. The coupling between the internal degrees of freedom of the two molecules makes up 11% of the total variation. Note that, in absolute terms, this corresponds to a variation of 40 kJ mol^{-1}. The smallest variation stems from arguably the most exotic term: the coupling of the external degrees of freedom of molecule 2 with respect to molecule 1 with themselves. However, although fractionally minor, this 1% percent of the span still makes up for 3.6 kJ mol^{-1}, a value that could have physical and biological significance.

It is of interest, especially in the context of rational drug design, to assess whether the above results hold if smaller molecules are involved. To investigate this, we have analyzed the relationship between different configurational entropy contributions normalized by the number of degrees of freedom ($3N - 6$, where N is the total number of atoms) for each binding process (Figure 3b). This normalization down-weights the binding contributions of larger complexes or, i.e., up-weights those of the smaller complexes. For this reason, Y, which is comprised of a small but constant number of six external degrees of freedom regardless of the size of the

DOI: 10.1021/acs.jctc.8b01254
J. Chem. Theory Comput. 2019, 15, 3844−3853

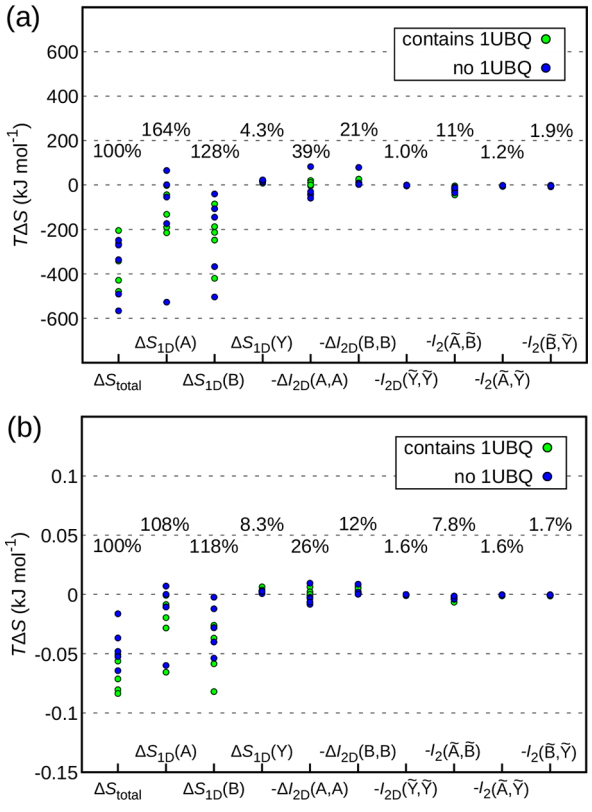

Figure 3. Contributions to configurational entropy change upon protein binding. Every column represents one of the contributions in eq 21, and every binding process contributes one data point in every column. The percentage values represent the span in the given column in relation to the span of the first column describing the total configurational entropy change. Green points denote complexes involving ubiquitin (Figure 1a), while blue points denote complexes not involving ubiquitin (Figure 1b). (b) Same as (a) but normalized by the number of degrees of freedom of the complex for each binding process, thus illustrating size dependence.

complex, gains in importance. This is reflected in $\Delta S_{1D}(Y)$ almost doubling. Also, the other terms involving Y tend to rather increase their impact [with the minor outlier $-I_{2D}(\tilde{B},\tilde{Y})$]. The fact that the smallest complex in this study is comprised of 1094 atoms together with the fact that the span of $\Delta S_{1D}(Y)$ increases already by a factor of 2 demonstrates the importance of these external degrees of freedom as well as all of their couplings when investigating small systems. Thus, from an entropic point of view, retaining as much rotational and translational freedom as possible at the binding site should turn out especially beneficial for small ligands such as many drug compounds. However, due to the enthalpy/entropy compensation,[20−22] one should also consider the impact on the enthalpic component of any practical optimization in this direction.

Note that there exists a fundamental arbitrariness in separating external from internal contributions, as already discussed by Gilson and co-workers.[31,39,40] In the BAT coordinate system,[12,23−28] this is reflected in the choice of root atoms from which the construction of the coordinate system is initiated. Accordingly, in the bound state, a nonphysical pseudobond is introduced connecting to the root atoms of the second molecule in order to form a complete coordinate system. For this reason, we numerically explore the impact of this largely arbitrary choice by performing our calculations for 5 different sets of root atoms in the second molecule for each of the 10 protein complexes. While Figure 3a illustrates the values chosen from the root atoms that minimize $\Delta S_{1D}(Y)$, as proposed in ref 31, Figure 5 shows the changes of

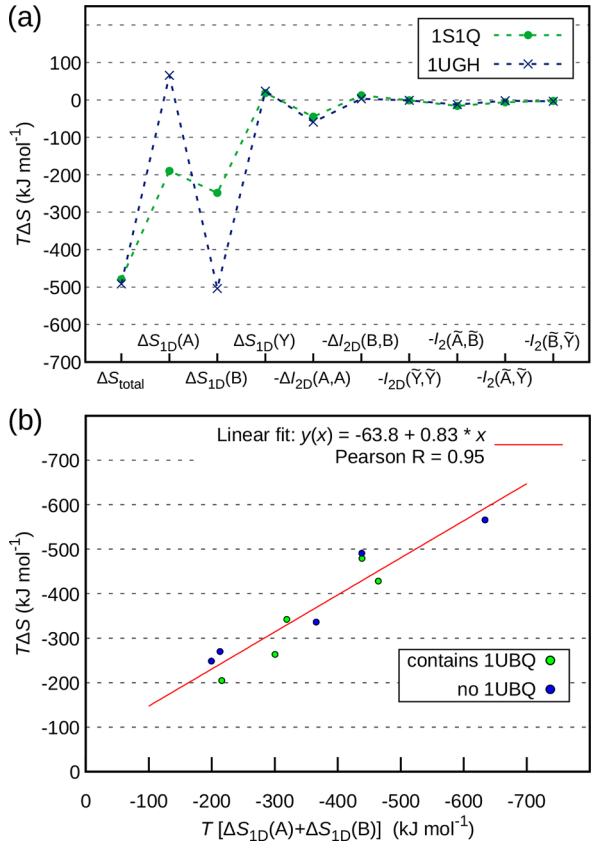

Figure 4. Relationship between different configurational entropy contributions. (a) Footprint of configurational entropy contributions for two specific complexes demonstrating the nonpredictable relationship between different terms. (b) The sum of the leading internal uncoupled terms is an excellent linear predictor of the total entropy change.

the values with respect to the maximization of such terms. The spans relative to the total entropy change in Figure 3a suggest that the global importance of the individual terms is hardly affected by this fundamental arbitrariness. However, individual terms can exhibit quite a drastic change for certain proteins.

Generally, the footprint of a given molecule does not follow a readily discernible pattern, which is illustrated in the case of the 1S1Q and 1UGH complexes in Figure 4a (see Figure 1 and Table 1 for further details). While the two complexes exhibit almost the same total entropy change ΔS_{total}, the contribution of the leading uncoupled terms ΔS_{1D} is vastly different. For 1S1Q, the two binding partners contribute similarly when it comes to ΔS_{1D}. In 1UGH, however, a small ΔS_{1D} contribution of the larger binding partner 1AKZ is accompanied by a large ΔS_{1D} contribution of the smaller binding partner 1UGI. Surprisingly, however, the rest of the terms are virtually the same, which is noteworthy especially when it comes to the internal coupling terms. Remarkably, however, the sum of the internal uncoupled terms $\Delta S_{1D}(A) + \Delta S_{1D}(B)$ exhibits an excellent linear correlation with the total entropy change for both the ubiquitin-containing and the non-ubiquitin-containing complexes (Figure 4b). This fact provides fundamental

DOI: 10.1021/acs.jctc.8b01254
J. Chem. Theory Comput. 2019, 15, 3844−3853

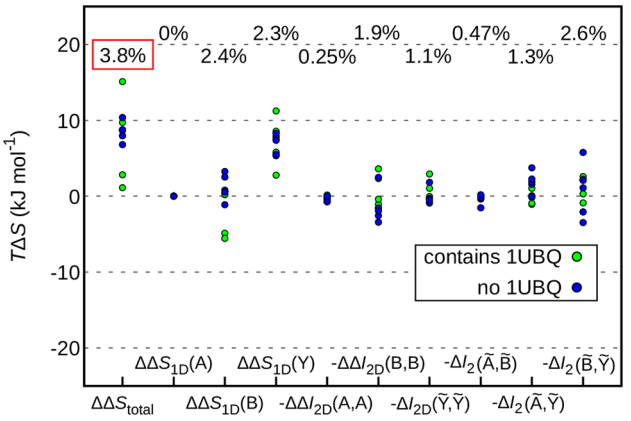

Figure 5. Effect of the choice of coordinate system on the importance of the entropy contributions. There is a largely arbitrary choice of root atoms to define the BAT coordinate system. Figure 3a shows values where the root atoms for each complex have been chosen (out of five sets of root atoms) in order to minimize $\Delta S_{1D}(Y)$. The current graph shows the changes relative to this minimum choice when root atoms are chosen in order to maximize $\Delta S_{1D}(Y)$. The percentage values describe the spans relative to the total entropy change in Figure 3a. Green points denote complexes involving ubiquitin (Figure 1a), while blue points denote complexes not involving ubiquitin (Figure 1b).

support for the recently developed NMR-based methods for measuring the configurational entropy change of protein interactions,[4,5,46,47] which critically rely on such linear behavior. Nevertheless, although the external as well as the coupling terms obviously average out to a constant fraction rather well, given the ranges in Figure 3a, a customized recalibration for the system of interest (as done by the NMR methods), may likely be required for improved accuracy.

4. CONCLUSIONS

In summary, we have presented here a comprehensive theoretical framework for analyzing different contributions to configurational entropy change over internal and external degrees of freedom. Moreover, we have provided a quantitative assessment of the individual contributions to configurational entropy change in the case of a large set of MD simulations of biomolecular binding processes. While the analytical parts of our study are exact, the latter analysis was subject to different sources of uncertainty, including force field errors and convergence issues, and its results should be treated as such. We hope that these efforts will help to complete the theoretical foundation used for treating the configurational entropy in biomolecular systems. With recent methodological advances on both experimental and computational fronts, it is our firm conviction that such a foundation will be instrumental in numerous fundamental and applied contexts alike.

5. METHODS

MD simulations were performed as described previously[36−38] using the GROMACS 4.0.7 simulation package,[48,49] the GROMOS 45A3 force field,[50] and the SPC water model.[51] Proteins were placed in water boxes, together with the necessary number of sodium or chloride counterions to reach neutrality, and subjected to energy minimization, followed by heating to 300 K for 100 ps and subsequent unconstrained MD simulations. The length of each MD trajectory was 1 μs, with the first 200 ns treated as an equilibration period and the remaining 800 ns analyzed. Simulations were carried out with a time step of 2 fs using 3D periodic boundary conditions, in the isothermal−isobaric (*NPT*) ensemble with an isotropic pressure of 1 bar and a constant temperature of 300 K, while system coordinates were output every 1 ps. The pressure and the temperature were controlled using the Berendsen thermostat and barostat[52] with 1.0 and 0.1 ps relaxation parameters, respectively, and a compressibility of 4.5×10^{-5} bar^{-1} for the barostat. Bond lengths were constrained using LINCS.[53] The van der Waals interactions were treated using a cutoff of 14 Å. Electrostatic interactions were evaluated using the reaction-field method,[54] with a direct sum cutoff of 14 Å and relative permittivity of 61. For the complex 1YD8, due to the lack of a separate structure, the ubiquitin binding partner (human GGA3 GAT domain) was extracted from the PDB structure of the complex and equilibrated for an additional 500 ns. The PARENT[36] program suite, a configurational entropy package in parallel architecture, was used for entropy calculations by applying the MIST approximation.[10,35] For sampling probability densities, 50 bins were used in one-dimensional cases and $50 \times 50 = 2500$ in two-dimensional cases.

■ ASSOCIATED CONTENT

Supporting Information

The Supporting Information is available free of charge on the ACS Publications website at DOI: 10.1021/acs.jctc.8b01254.

Convergence analysis from shuffled trajectories of the same three representative complexes as in the main article (PDF)

■ AUTHOR INFORMATION

Corresponding Author

*E-mail: bojan.zagrovic@univie.ac.at.

ORCID

Markus Fleck: 0000-0002-8648-2164

Bojan Zagrovic: 0000-0003-3814-3675

Notes

The authors declare no competing financial interest.

■ ACKNOWLEDGMENTS

We thank Anton A. Polyansky and other members of the Laboratory of Computational Biophysics at the University of Vienna for useful advice and critical reading of the manuscript. Funding by the European Research Council (Starting Independent Grant 279408 to B.Z.) and Austrian Science Fund FWF (Standalone Grant P 30550 to B.Z.) is gratefully acknowledged.

■ REFERENCES

(1) Wodak, S. J.; Janin, J. Structural basis of macromolecular recognition. *Adv. Protein Chem.* **2002**, *61*, 9−73.

(2) Chandler, D. *Introduction to modern statistical mechanics*; Oxford University Press: New York, 1987.

(3) Frederick, K. K.; Marlow, M. S.; Valentine, K. G.; Wand, A. J. Conformational entropy in molecular recognition by proteins. *Nature (London, U. K.)* **2007**, *448*, 325−329.

(4) Marlow, M. S.; Dogan, J.; Frederick, K. K.; Valentine, K. G.; Wand, A. J. The role of conformational entropy in molecular recognition by calmodulin. *Nat. Chem. Biol.* **2010**, *6*, 352−358.

(5) Tzeng, S.-R.; Kalodimos, C. G. Protein activity regulation by conformational entropy. *Nature (London, U. K.)* **2012**, *488*, 236−240.

DOI: 10.1021/acs.jctc.8b01254
J. Chem. Theory Comput. 2019, 15, 3844−3853

(6) Schlitter, J. Estimation of absolute and relative entropies of macromolecules using the covariance matrix. *Chem. Phys. Lett.* **1993**, *215*, 617−621.
(7) Polyansky, A. A.; Zubac, R.; Zagrovic, B. In *Computational Drug Discovery and Design*; Baron, R., Ed.; Springer New York: New York, 2012; Vol. *819*; pp 327−353.
(8) Numata, J.; Wan, M.; Knapp, E.-W. Conformational entropy of biomolecules: beyond the quasi-harmonic approximation. *Genome Inform* **2007**, *18*, 192−205.
(9) Numata, J.; Knapp, E.-W. Balanced and Bias-Corrected Computation of Conformational Entropy Differences for Molecular Trajectories. *J. Chem. Theory Comput.* **2012**, *8*, 1235−1245.
(10) King, B. M.; Silver, N. W.; Tidor, B. Efficient Calculation of Molecular Configurational Entropies Using an Information Theoretic Approximation. *J. Phys. Chem. B* **2012**, *116*, 2891−2904.
(11) Killian, B. J.; Kravitz, J. Y.; Somani, S.; Dasgupta, P.; Pang, Y.-P.; Gilson, M. K. Configurational Entropy in Protein-Peptide Binding: Computational Study of Tsg101 Ubiquitin E2 Variant Domain with an HIV-Derived PTAP Nonapeptide. *J. Mol. Biol.* **2009**, *389*, 315−335.
(12) Killian, B. J.; Yundenfreund Kravitz, J.; Gilson, M. K. Extraction of configurational entropy from molecular simulations via an expansion approximation. *J. Chem. Phys.* **2007**, *127*, 024107.
(13) Karplus, M.; Kushick, J. N. Method for estimating the configurational entropy of macromolecules. *Macromolecules* **1981**, *14*, 325−332.
(14) Hnizdo, V.; Tan, J.; Killian, B. J.; Gilson, M. K. Efficient calculation of configurational entropy from molecular simulations by combining the mutual-information expansion and nearest-neighbor methods. *J. Comput. Chem.* **2008**, *29*, 1605−1614.
(15) Hnizdo, V.; Darian, E.; Fedorowicz, A.; Demchuk, E.; Li, S.; Singh, H. Nearest-neighbor nonparametric method for estimating the configurational entropy of complex molecules. *J. Comput. Chem.* **2007**, *28*, 655−668.
(16) Andricioaei, I.; Karplus, M. On the calculation of entropy from covariance matrices of the atomic fluctuations. *J. Chem. Phys.* **2001**, *115*, 6289.
(17) Di Nola, A.; Berendsen, H. J. C.; Edholm, O. Free energy determination of polypeptide conformations generated by molecular dynamics. *Macromolecules* **1984**, *17*, 2044−2050.
(18) Levy, R. M.; Karplus, M.; Kushick, J.; Perahia, D. Evaluation of the configurational entropy for proteins: application to molecular dynamics simulations of an Î±-helix. *Macromolecules* **1984**, *17*, 1370−1374.
(19) Steinberg, I. Z.; Scheraga, H. A. Entropy Changes Accompanying Association Reactions of Proteins. *J. Biol. Chem.* **1963**, *238*, 172−181.
(20) Garbett, N. C.; Chaires, J. B. Thermodynamic studies for drug design and screening. *Expert Opin. Drug Discovery* **2012**, *7*, 299−314.
(21) Freire, E. Do enthalpy and entropy distinguish first in class from best in class? *Drug Discovery Today* **2008**, *13*, 869−874.
(22) Du, X.; Li, Y.; Xia, Y.-L.; Ai, S.-M.; Liang, J.; Sang, P.; Ji, X.-L.; Liu, S.-Q. Insights into Protein-Ligand Interactions: Mechanisms, Models, and Methods. *Int. J. Mol. Sci.* **2016**, *17*, 144.
(23) Potter, M. J.; Gilson, M. K. Coordinate Systems and the Calculation of Molecular Properties. *J. Phys. Chem. A* **2002**, *106*, 563−566.
(24) Chang, C.-E.; Potter, M. J.; Gilson, M. K. Calculation of Molecular Configuration Integrals. *J. Phys. Chem. B* **2003**, *107*, 1048−1055.
(25) Pitzer, K. S. Energy Levels and Thermodynamic Functions for Molecules with Internal Rotation: II. Unsymmetrical Tops Attached to a Rigid Frame. *J. Chem. Phys.* **1946**, *14*, 239.
(26) Herschbach, D. R.; Johnston, H. S.; Rapp, D. Molecular Partition Functions in Terms of Local Properties. *J. Chem. Phys.* **1959**, *31*, 1652.
(27) Go, N.; Scheraga, H. A. On the Use of Classical Statistical Mechanics in the Treatment of Polymer Chain Conformation. *Macromolecules* **1976**, *9*, 535−542.
(28) Parsons, J.; Holmes, J. B.; Rojas, J. M.; Tsai, J.; Strauss, C. E. M. Practical conversion from torsion space to Cartesian space for in silico protein synthesis. *J. Comput. Chem.* **2005**, *26*, 1063−1068.
(29) Gohlke, H.; Case, D. A. Converging free energy estimates: MM-PB(GB)SA studies on the protein-protein complex Ras-Raf. *J. Comput. Chem.* **2004**, *25*, 238−250.
(30) Zoete, V.; Meuwly, M.; Karplus, M. Study of the insulin dimerization: Binding free energy calculations and per-residue free energy decomposition. *Proteins: Struct., Funct., Genet.* **2005**, *61*, 79−93.
(31) Zhou, H.-X.; Gilson, M. K. Theory of Free Energy and Entropy in Noncovalent Binding. *Chem. Rev.* **2009**, *109*, 4092−4107.
(32) Matsuda, H. Physical nature of higher-order mutual information: Intrinsic correlations and frustration. *Phys. Rev. E: Stat. Phys., Plasmas, Fluids, Relat. Interdiscip. Top.* **2000**, *62*, 3096−3102.
(33) Baranyai, A.; Evans, D. J. Direct entropy calculation from computer simulation of liquids. *Phys. Rev. A: At., Mol., Opt. Phys.* **1989**, *40*, 3817−3822.
(34) Fenley, A. T.; Killian, B. J.; Hnizdo, V.; Fedorowicz, A.; Sharp, D. S.; Gilson, M. K. Correlation as a Determinant of Configurational Entropy in Supramolecular and Protein Systems. *J. Phys. Chem. B* **2014**, *118*, 6447−6455.
(35) King, B. M.; Tidor, B. MIST: Maximum Information Spanning Trees for dimension reduction of biological data sets. *Bioinformatics* **2009**, *25*, 1165−1172.
(36) Fleck, M.; Polyansky, A. A.; Zagrovic, B. PARENT: A Parallel Software Suite for the Calculation of Configurational Entropy in Biomolecular Systems. *J. Chem. Theory Comput.* **2016**, *12*, 2055−2065.
(37) Polyansky, A. A.; Kuzmanic, A.; Hlevnjak, M.; Zagrovic, B. On the Contribution of Linear Correlations to Quasi-harmonic Conformational Entropy in Proteins. *J. Chem. Theory Comput.* **2012**, *8*, 3820−3829.
(38) Fleck, M.; Polyansky, A. A.; Zagrovic, B. Self-Consistent Framework Connecting Experimental Proxies of Protein Dynamics with Configurational Entropy. *J. Chem. Theory Comput.* **2018**, *14*, 3796.
(39) Chang, C.-E.; Gilson, M. K. Free Energy, Entropy, and Induced Fit in Host-Guest Recognition: Calculations with the Second-Generation Mining Minima Algorithm. *J. Am. Chem. Soc.* **2004**, *126*, 13156−13164.
(40) Gilson, M. K.; Given, J. A.; Bush, B. L.; McCammon, J. A. The statistical-thermodynamic basis for computation of binding affinities: a critical review. *Biophys. J.* **1997**, *72*, 1047−1069.
(41) Berman, H. M.; Westbrook, J.; Feng, Z.; Gilliland, G.; Bhat, T. N.; Weissig, H.; Shindyalov, I. N.; Bourne, P. E. The Protein Data Bank. *Nucleic Acids Res.* **2000**, *28*, 235−242.
(42) Berman, H.; Henrick, K.; Nakamura, H. Announcing the worldwide Protein Data Bank. *Nat. Struct. Mol. Biol.* **2003**, *10*, 980−980.
(43) Hnizdo, V.; Gilson, M. K. Thermodynamic and Differential Entropy under a Change of Variables. *Entropy* **2010**, *12*, 578−590.
(44) Landau, L. D.; Lifshitz, E. M. *Statistical physics, Part 1*, 3rd ed.; Course of theoretical physics; Elsevier, 1980; Vol. *5*.
(45) Cover, T. M.; Thomas, J. A. *Elements of information theory*, 2nd ed.; Wiley-Interscience: Hoboken, NJ, 2006.
(46) Caro, J. A.; Harpole, K. W.; Kasinath, V.; Lim, J.; Granja, J.; Valentine, K. G.; Sharp, K. A.; Wand, A. J. Entropy in molecular recognition by proteins. *Proc. Natl. Acad. Sci. U. S. A.* **2017**, *114*, 6563−6568.
(47) Kasinath, V.; Sharp, K. A.; Wand, A. J. Microscopic Insights into the NMR Relaxation-Based Protein Conformational Entropy Meter. *J. Am. Chem. Soc.* **2013**, *135*, 15092−15100.
(48) Berendsen, H.; van der Spoel, D.; van Drunen, R. GROMACS: A message-passing parallel molecular dynamics implementation. *Comput. Phys. Commun.* **1995**, *91*, 43−56.
(49) Abraham, M. J.; Murtola, T.; Schulz, R.; Páll, S.; Smith, J. C.; Hess, B.; Lindahl, E. GROMACS: High performance molecular

DOI: 10.1021/acs.jctc.8b01254
J. Chem. Theory Comput. 2019, 15, 3844−3853

simulations through multi-level parallelism from laptops to supercomputers. *SoftwareX* **2015**, *1−2*, 19−25.
(50) Schuler, L. D.; Daura, X.; van Gunsteren, W. F. An improved GROMOS96 force field for aliphatic hydrocarbons in the condensed phase. *J. Comput. Chem.* **2001**, *22*, 1205−1218.
(51) Berendsen, H. J. C.; Postma, J. P. M.; van Gunsteren, W. F.; Hermans, J. *Intermolecular Forces; The Jerusalem Symposia on Quantum Chemistry and Biochemistry*; Springer: Dordrecht, The Netherlands, 1981; pp 331−342.
(52) Berendsen, H. J. C.; Postma, J. P. M.; van Gunsteren, W. F.; DiNola, A.; Haak, J. R. Molecular dynamics with coupling to an external bath. *J. Chem. Phys.* **1984**, *81*, 3684.
(53) Hess, B.; Bekker, H.; Berendsen, H. J. C.; Fraaije, J. G. E. M. LINCS: A linear constraint solver for molecular simulations. *J. Comput. Chem.* **1997**, *18*, 1463−1472.
(54) Tironi, I. G.; Sperb, R.; Smith, P. E.; van Gunsteren, W. F. A generalized reaction field method for molecular dynamics simulations. *J. Chem. Phys.* **1995**, *102*, 5451.

DOI: 10.1021/acs.jctc.8b01254
J. Chem. Theory Comput. 2019, 15, 3844−3853